Conventional and Geogrid-encased Stone Piles Improved Soft Ground under an Embankment

Mohamed B. D. Elsawy

Assistant Professor of Department of Civil Engineering,
Faculty of Engineering, University of Aswan, Aswan, Egypt.
e-mail: mohamedelsawy75@ymail.com.

ABSTRACT

Stone piles technique have been effectively utilized in soft soil to increase the bearing capacity and accelerates the consolidation. To improve the reinforcement and the drainage functions of the stone piles, the geosynthetic are used as encasement. In the current research, a case history of an embankment constructed on the reinforced soft soil with conventional stone piles has been chosen to be simulated. 3-Dimension, plane strain and axisymmetric techniques are used to simulate the embankment parts. The stone piles are reinforced by geogrid material to imply the influence of the encasement on the behavior of the stone piles-soft soil foundation. The consolidation analysis is applied to investigate the long-term behavior of the clay. There is a good agreement between the FEM results and the field measurements of the reinforced soft soil with conventional stone piles. The 3D and the axisymmetric models induce better agreement with field measurements than that of the plane strain model. The reinforced soft soil with encased stone pile has a smaller settlement and a shorter consolidation time than those of the reinforced soft soil with conventional stone piles. The reduction in the settlement is more significant with developing consolidation time. The dissipation of the excess pore water pressure in the reinforced clay with encased pile consumes shorter time in comparison with the reinforced clay with conventional piles. The effective vertical stress and the stress concentration in the encased piles are higher than those in the conventional piles. The encasement also causes reduction in the total stress of the surrounding clay which participates in the acceleration of the consolidation

KEYWORDS: Stone piles; Geogrid; Settlement; Consolidation

INTRODUCTION

Embankments constructed on soft deposits sustains problems such as base failure, excessive settlement, large lateral deformation, and local or global instability. Stone piles are increasingly used as an effective ground improvement method to support a wide variety of structures, including buildings and embankments (Balaam and Booker 1985; Borges 2009; Murugesan and Rajagopal 2010; Mokhtari and Kalantari 2012). Stone piles accelerate consolidation of soft soil resulting from the generated lateral drainage paths, increased load-bearing capacity, and reduced settlement (Bergado and Long 1994; Chandrawanshi et al. 2016). The bearing capacity of stone piles depends mainly on the lateral support from the shear strength of the surrounding soil. If lateral support is not sufficient, the stone piles sustain excessive settlement and they may fails by lateral bulging.

Therefore, construction of stone piles in soft soils with undrained strength (Su) less than 15 kPa is almost impossible, however, because of the lack of lateral support, (FHWA 1980).

Encasing stone piles with geosynthetics was recommended to enhance the lateral pile confinement which resulting on increasing load-bearing capacity. Additionally, encasement prevents the lateral squeezing of stones into the surrounding soil and vice versa. The effectiveness of geosynthetic encasement on the bearing capacity and settlement response of composite ground has been studied in laboratory and small-scale model tests (Murugesan and Rajagopal 2007; Gniel and Bouazza 2010; Das and Pal 2013; Ab Aziz et al. 2015). Successful numerical studies of encased stone piles can also be found in the literature. These analyses have historically been performed assuming either plane strain (e.g., Tan et al. 2008; Deb 2010) or axisymmetric (e.g., Tan et al. 2008; Borges et al. 2009; Elsawy 2013; Marto et al. 2013; Ng and Tan 2014; Hosseinpour et al. 2015; Khabbazian et al. 2015) idealizations. The concept of a ‘‘unit cell’’, as axisymmetric idealization, has been the most popular approach for numerically simulating response of either conventional or encased stone piles reinforced soft soil under embankments. While the 3D Modelling of embankments on conventional and encased stone pile reinforcing soft soil is very limited in the past research (Khabbazian et al. 2015). Additionally, Comparison between the 3D, unit cell and plain strain models wasn't studied by the past researchers. With regards to the practical applications of stone piles under embankment with field measurements were done by (Tan et al. 2008; Almeida et al. 2014). Additionally, Raithel et al. (2002) also cited many successful case histories of geotextile-encased granular columns (GECs) under embankment in Germany, Sweden, and the Netherlands of the use of GECs for the stabilization of embankments on soft soils.

In the current research a case history of an embankment was chosen from the past research. The embankment constructed on reinforced soft soil with conventional stone piles has been numerically simulated with 3D, unit cell and plain strain models. The results of the field measurements and the numerical analyses were compared. The simulation of the embankment construction on reinforced soft soil with encased stone piles has also been done utilizing 3D and unit cell models. The consolidation behavior of this system is investigated to study the performance of the geogrid-encasement in the reinforced soil during and after consolidation. The results of the used three models have been compared considering settlement, excess pore water pressure, and stresses in the piles and in the soil.

CASE HISTORY DESCRIPTION

An embankment, located in Penchala Toll Plaza project at New Pantai Expressway, Malaysia, was adapted for the FEM simulation. A brief description of the project was given by Tan et al. (2008). The embankment geometry with the stone pile reinforced soft profile is shown in Fig. 1 having a line of symmetry on the left boundary. The embankment with 40 m wide and 1.8 m height is filled by sandy material. The embankment has a slope of 2 horizontal to 1 vertical. The stone piles have a diameter of 0.8 m and a spacing distance between piles of 2.4 m. The stone piles, arranged in a square grid, extend through the soft soil for a depth of 6 m above the layer of the stiff clay. The upper crust layer is 1 m thick fill for strong soil. This layer was provided as a replacement of soft-clay surface to improve the ground for a stable construction platform as well as drainage of water during consolidation. The groundwater level is one meter below the ground surface. Two settlement plates (SP1 and SP2), as shown in Fig. 1, were installed in situ to measure the settlement at the center of the embankment and at 8 m from its toe. The excess pore water pressure was calculated at points A and B which located at a depth of 3.5 m. The points A and B have a horizontal distance of 1.2 m and 22 m far from the centerline of the embankment, respectively.

NUMERICAL MODELING AND SELECTION OF PARAMETERS

2D and 3D modellings are utilized to simulate the embankment construction. Mohr-coulomb model is used to describe all soils, soft soil, stone piles, crust layer, embankment fill and stiff clay, which is considered realistic approximations of the soils. The used parameters are depicted in Table 1. All the soils are modelled in drained conditions except the soft clay is modelled in undrained conditions. The project involved rapid embankment construction. The stone piles first installed by partial soil replacement. Then, the construction of the embankment was done three equal layers (0.6 m increment in embankment height in each layer). Each layer of the embankment is constructed with 3 days consolidation period, giving altogether 9 days. The consolidation process has been then continued with no change in loading condition until the remaining excess pore water pressure fell below a specified near zero value (1 kPa), which reach the end of the simulation.

The stone piles are assumed to be encased with Combigrid 40/40 Q1 (Naue GmbH). The composite geogrid/non-woven geotextile is a geogrid covered by a geotextile to allow drainage without mixing soft soil with stone particles, as illustrated in Fig. 2-c. The geotextile is arranged in such a way that it would not contribute either to the vertical or radial stiffness of the encased stone pile. The geogrid encasement is modeled as a linear elastic continuum element with a series of one-dimensional bare (line) elements having no bending stiffness, using flexible elastic elements which can mobilize only axial tension forces. The elastic parameter used in modelling the geogrid encasement with Plaxis program is only the axial stiffness J = EA (forces per unit width per unit strain). The encasement is subjected to axial extension, and there are no other deformations: therefore the Poisson's ratio of the encasement equals zero. The geogrid stiffness (J = EA) is calculated at a strain of 2 % where geogrid is under working stress conditions. The used geogrid has a stiffness of J = 800 kN/m. No interaction between the geogrid and the surrounding soil was assumed in the current study. This is because no slippage occurs between the geogrid and the surrounding soil, Elsawy (2013).

Table 1: Material parameters for embankment models

Material	Unsaturated Density, γ_{us} (kN/m³)	Saturated Density, γ_{sa} (kN/m³)	ν	E (kPa)	k_h (m/s)	k_v (m/s)	ć (kPa)	φ́ (deg)
Embank-ment Fill	18	20	0.3	15,000	1.16 x 10-5	1.16 x 10-5	3	33
Crust	17	18	0.3	15,000	3.47 x10-7	1.16 x 10-7	3	28
Soft clay	15	15	0.3	1,100	3.47 x10-9	1.16 x 10-9	1	20
Stiff clay	18	20	0.3	40,000	3.47 x10-9	1.16 x 10-9	3	30
Stone pile	19	20	0.3	30,000	1.16 x10-4	1.16 x10-4	5	40

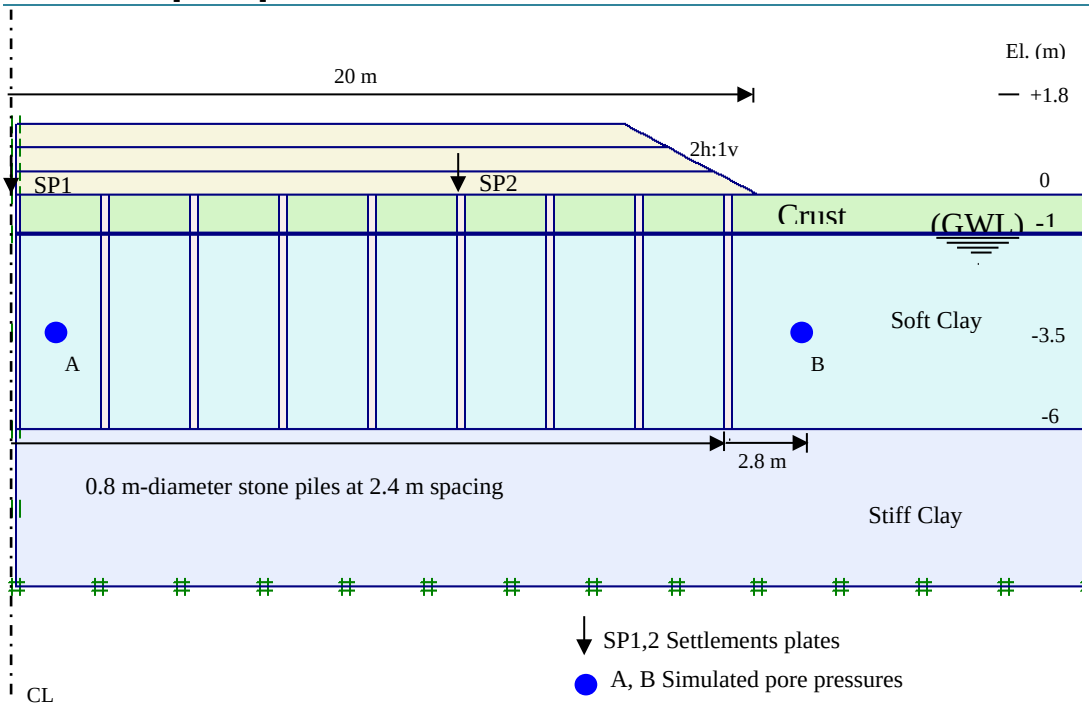

Figure 1: Cross section of embankment case history through centreline of stone piles

2D Modelling

The plane-strain modelling is possible as the embankment extended to a distance of more than 200 m with approximately uniform cross-sectional geometry. Hence, in the current study the plane-strain modelling has been done by Plaxis 2D Version 8.1 using width of the stone piles (or walls) of 0.21 m and spacing distance of 2.4 m, as illustrated in Fig. 1. The plane-strain pile width is given by the following relationship based on the equivalence area of the replacement ratio:

$$b_c = B\,(r_c^2 / r_e^2) \qquad (1)$$

where b_c is the half width of the wall, B = (S/2) is the half of the spacing distance between piles, r_c = (d/2) is the radius of the stone pile and r_e = (d_e/2) is the radius of the drainage zone or the unit cell which is equivalent to the plane strain width. Where is in square orientation r_e = 1.13 B, as shown in Fig. 2-a.

The unit cell technique has been also used in this study to simulate the embankment using axisymmetric model in Plaxis 2D. The unit cell consists of a stone pile and the surrounding soft soil over the stiff clay, as shown in Figs. 2-a and 2-b. The stone piles are installed in square panels which produces an equivalent unit cell with a diameter of 2.72 m (1.13 x 2.4 m). In 2D modelling (the plain strain and the axisymmetric models), half of the model is simulated utilizing medium mesh with 15-node wedge elements. The horizontal and the vertical displacements are restrained in the bottom boundaries while the horizontal displacement is only restrained in the lateral boundaries.

3D Modelling

Full 3D model was developed to understand the long-term behaviour of stone piles and geogrid-encased stone piles-reinforced ground. The commercial FE package PLAXIS 3D (2012) was used for the modelling. Half of the model is simulated as shown in Figure 3. Relatively medium mesh arrangements were used. The mesh was refined in the region of the pile soil interface to increase the accuracy of the predictions.

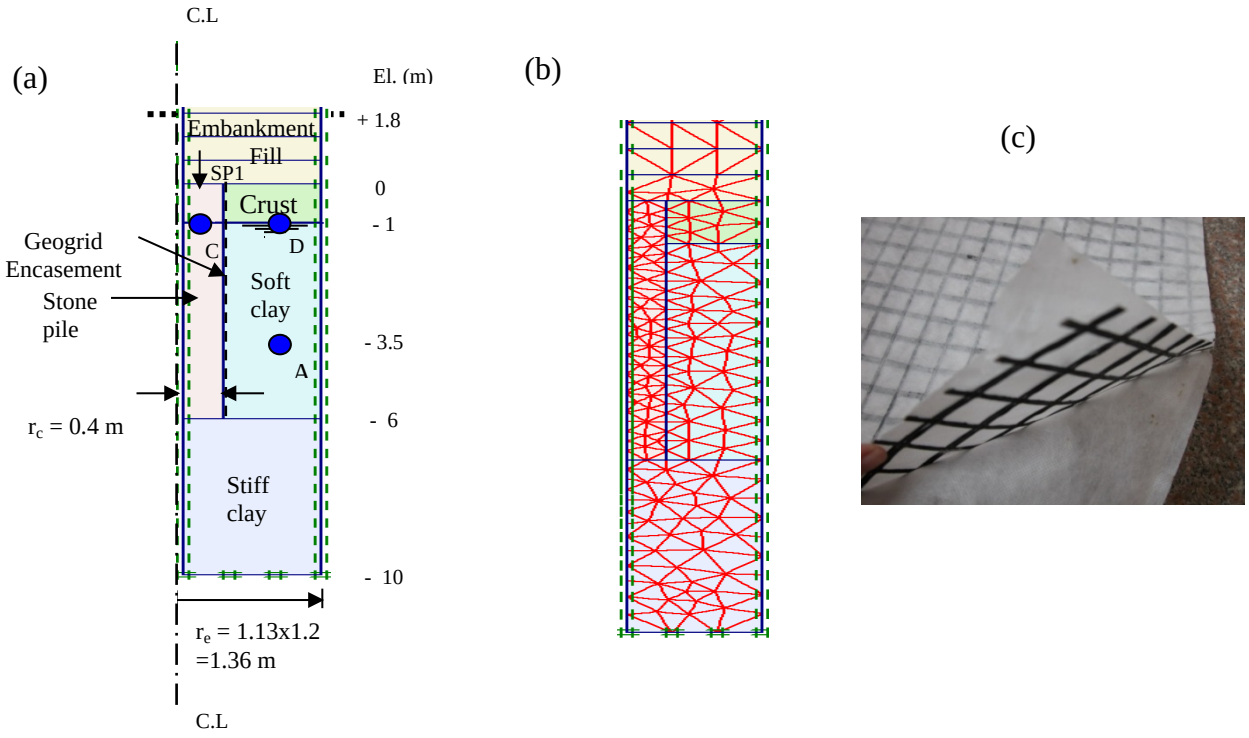

Figure 2: Unit cell (a) Model Parts (b) Finite element mesh (c) Composite of geogrid/geotextile

As displacement boundary is concerns, no displacements in the directions perpendicular to the symmetry planes and to the base were allowed. For the hydraulic boundary condition, the phreatic level was set at the top surface of the soft clay layer to generate a hydrostatic pore water pressure profile in the domain. A zero pore pressure boundary condition was applied at the top. The left boundary was assumed impervious to consider the fact that no flow entered to the symmetry plane. Since the right boundary was too far from the embankment to have significant influence on the results, it was set impervious. The finite element mesh was built using 10 node tetrahedral elements to represent soils, stone pile, and embankment fill. The geosynthetic reinforcement was modelled as geogrid element available in PLAXIS 3D, composed of 6 node triangular surface elements. Mohr-coulomb failure criterion was adopted for stone piles, embankment fill, and soils having linearly elastic perfectly plastic behaviour. After generation of initial stress and pore water pressure, stone piles were modelled by replacing soft soil element with stone pile, and the geosynthetic reinforcement was added as wished in place.

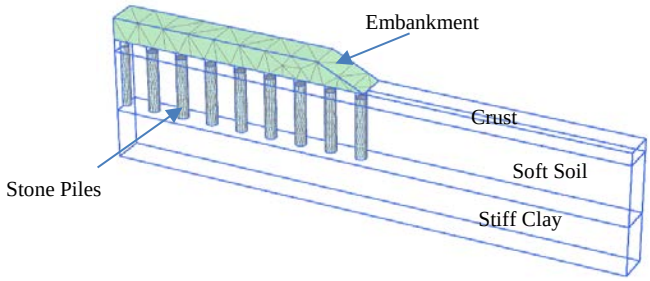

Figure 3: Full 3D model of the embankment constructed on stone piles reinforced soft soil

RESULTS AND DISCUSSIONS

The results of the numerical analyses having different modelling are compared to the field measurements of the settlement at SP1 and SP2. Additionally, the results of the excess pore water pressure from the current numerical analyses are compared to the results from 3D modeling of Tan et al. (2008) at point A and B. Tan et al. (2008) also simulated the embankment parts by the Plaxis 3D Tunnel Version 2 using 15-node wedge elements. Owing to the software limitations, the stone piles in three dimensional model were given as equivalent geometry with square cross-sectional area in place of the actual circular geometry.

Settlement

The settlement was calculated at SP1 in the 3D, in the plane strain and in the unit cell models to compare their results with the field measurements. Fig. 4 shows the relationship of the settlement with time for the field data and the models of the embankment at SP1. The settlement increases with time with rapid rate until the time reaches approximately 35 days. After that time, the settlement increases along time with a very small rate. The settlement hasn't approximately any increase after the time of 90 days. This means that the consolidation finished. There is a good agreement between the FEM results and the field measurements. The plane strain model induces settlement more than the field measurement. In the other hand, the 3D model and the unit cell model for the conventional stone piles imply settlement very close to the field settlement. Hence, the 3D and the axisymmetric model induce better agreement with field measurements than that of the plane strain model. The stone piles are encased with geogrid material which has a Stiffness of J = 800 kN/m. The embankment over the reinforced soil with encased stone piles is also modelled by the 3D and the unit cell models. The reinforced soft soil with encased stone pile has a settlement smaller than that of the reinforced soft soil with conventional stone pile. Fig. 4 shows also that the consolidation settlement is accelerated when encasing the stone piles. The 3D and the unit cell models induce a very good agreement for the settlement not only in the reinforced soil with conventional piles but also in the reinforced ground with encased piles.

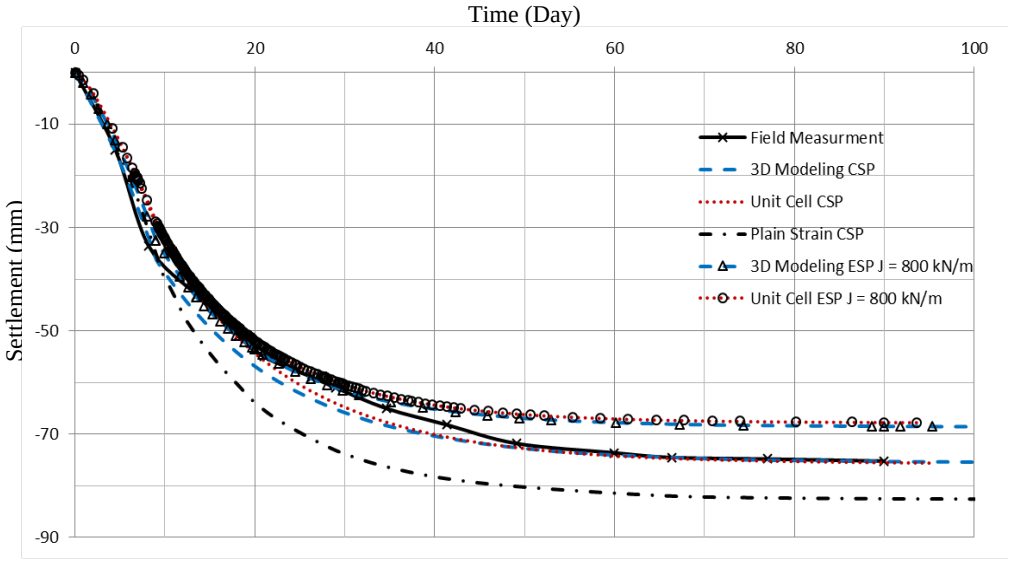

Figure 4: Time – settlement relationships for field measurements and numerical analyses

Figs. 5 and 6 show the settlement along the horizontal distance from the embankment centreline after 20 days and 90 days since the embankment has been constructed, respectively. The field measurements are compared with the FEM models. The measured settlement at SP1 and SP2 is approximately the same which leads to that the settlement under the embankment is constant. The constant settlement is well agreed by the 3D modelling after both times of 20 days and 90 days. While the plane strain model induces an overestimation for the field settlement after 20 and 90 days. The 3D and the plane strain models also predict the settlement distribution under the entire embankment. Beyond the embankment toe, the settlement converts to heave. The heave decreases with increasing time in which the two models are well agreed. When the stone piles are encased by geogrid material, a reduction only in the settlement occurs after 90 day from the construction. In the other hand, there is no significant reduction in the settlement after 20 days from construction. Therefore, the encasement has a greater influence on the settlement reduction after the consolidation in comparison with the period directly after the construction. This phenomenon is due to the encasement increases the pile stiffness resulting in increase the stress transfer and stress concentration in the piles during the consolidation. In the other hand, the reinforced soft soil with encased piles causes a slight reduction in the settlement. The reasons of that are the applied load and the encasement stiffness are somewhat small.

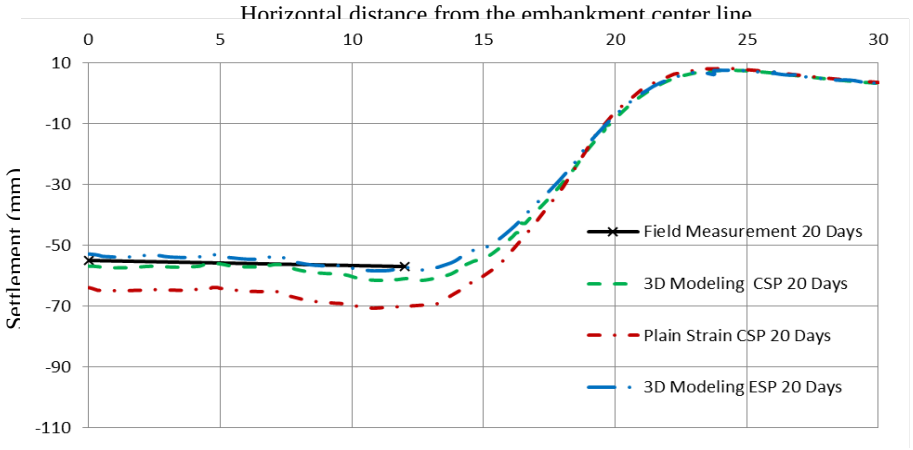

Figure 5: Surface settlement at time 20 days after construction

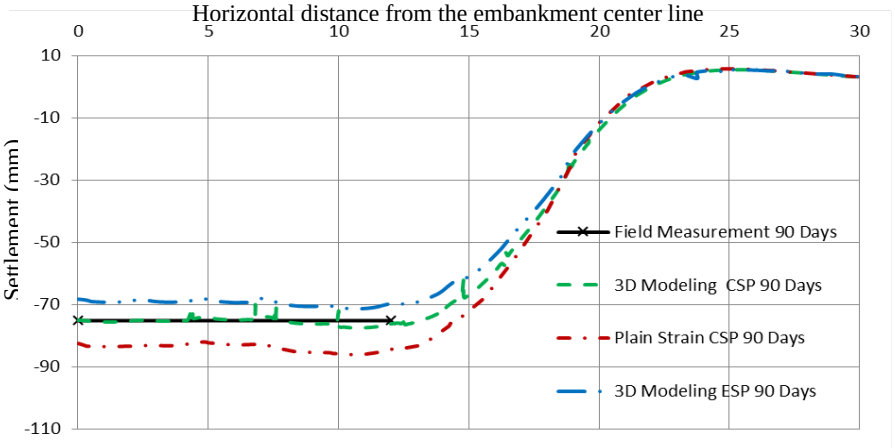

Figure 6: Surface settlement at time 90 days after construction

Excess pore water pressure

The excess pore water pressure was calculated from the 3D and the Plane strain model at locations A and B compared with the 3D simulation from the study of Tan et al. (2008). In the axisymmetric model, the excess pore water pressure was only calculated from at point A. Fig. 7-a and Fig. 7-b show the simulated excess pore water pressure with time at locations A and B, respectively. The excess pore water pressure at A in the models has an initial peak value of approximately 17 kPa due to the embankment construction and then dissipates with different rates to nearly zero after 90 days. The 3D model, the plane strain model and the unit cell model induce somewhat lower values of the excess pore water pressure than those of Tan et al (2008). In general, the models have good agreement between them. In the other hand, when the piles are encased with geogrid material, the dissipation of the excess pore pressure is slightly accelerated. This is more pronounced in the unit cell model as depicted in Fig. 7-a. The slight acceleration is because of the applied loads are small. It is expected that, the improvement in the production and in the dissipation of the excess pore presses will occur with increasing applied loads.

On the other side, at point B, 2 m away from the embankment edge, the excess pore water pressure was calculated by the 3D and plane strain models. The two models show a good agreement for the distribution of the excess pore water pressure with the results of 3D simulation of Tan et al. 2008. The excess pore water pressure has significantly lower peak values due to the diminished effects of the embankment loading and dissipates almost identically in the models. This means that the excess pore water pressure discrepancies are only confined within a distance of several meters from the stone piles. The excess pore water pressure here takes much longer than 120 days to dissipate and hence the acceleration of consolidation by the stone piles is hardly evident at this location. Additionally, the pile encasement has a very weak effect on the excess pore water pressure of the soil as illustrated in Fig. 7-b.

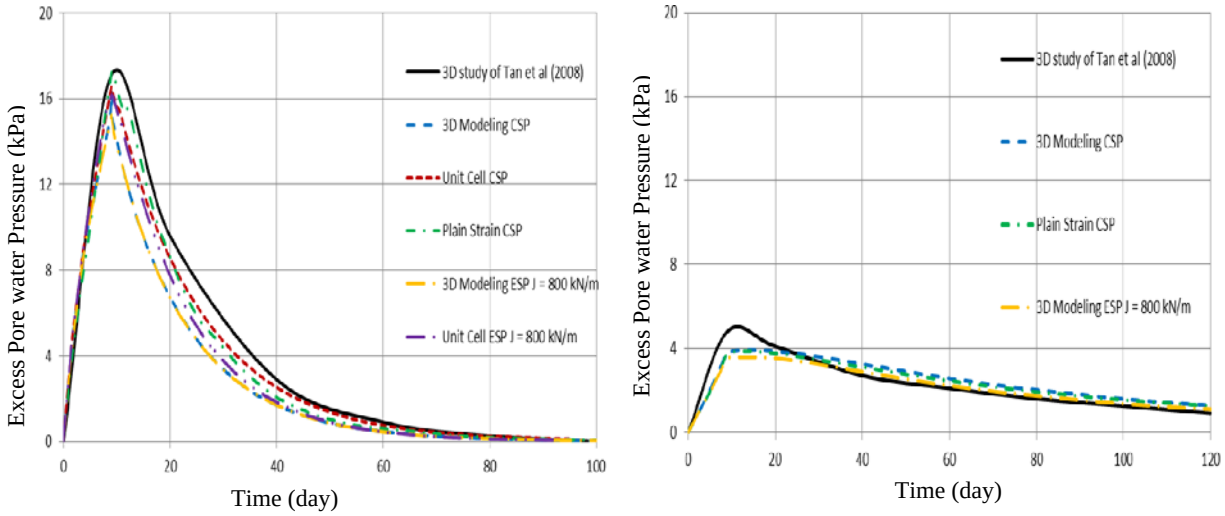

Figure 7: Excess pore water pressure values at (a) Point A and (b) Point B

Stress

The vertical effective stress and the stress concentration ratio were calculated at a depth of 1.0 in the top of the stone pile and in the surrounding soft soil for the models of 3D, unit cell and plain strain. Figs. 8-a and 8-b shows the effective vertical stress along the consolidation time in the conventional and the encased stone piles, and in the surrounding soil, respectively. The trends of the effective stress of the conventional and the encased stone piles are approximately similar. The developments of the effective stress with time in the reinforced clays are also approximately similar. The unit cell and plain strain models imply close results of the effective vertical stress and stress concentration ratio in both piles and soil. While the 3D model induces distant values in comparison with the other models.

The effective vertical stress in the encased stone piles is higher than that in the conventional stone piles. In contrast, the encasement of the stone pile causes reduction in the effective stress in the surrounding soft soil. This is pronounced in the 3D and the unit cell models. Additionally, beyond the yield point in the effective stress of the pile, the conventional piles induce somewhat softening while the encased piles imply somewhat hardening. Vice versa occurred in the surrounding soil, beyond the yield point of the effective stress, using conventional piles induces somewhat hardening while utilizing encased piles implies somewhat softening. These results agree with the study results of Almeida et al (2014). This phenomenon is due to the stress transfer from the surrounding soft soil to the encased stone pile. The increase in the stiffness of the overall encased stone pile leads to increase the stress concentration in the pile and to increase also the stress transfer from the surrounding soil, as depicted in Fig. 9. The development of the stress concentration ratio is similar to that of the effective stress. 3D model implies greater values of stress concentration ratio for the reinforced soil with both the conventional and encased pile compared with 2D models. These results agree with the study of Ng and Tan (2014). The stress concentration values are ranged from 3 to 5 which agreed with values from field measurement and past studies (range from 2 to 9). The stress concentration phenomenon has an important role in reducing consolidation settlement, accelerating consolidation time and increasing bearing capacity of the reinforced soil.

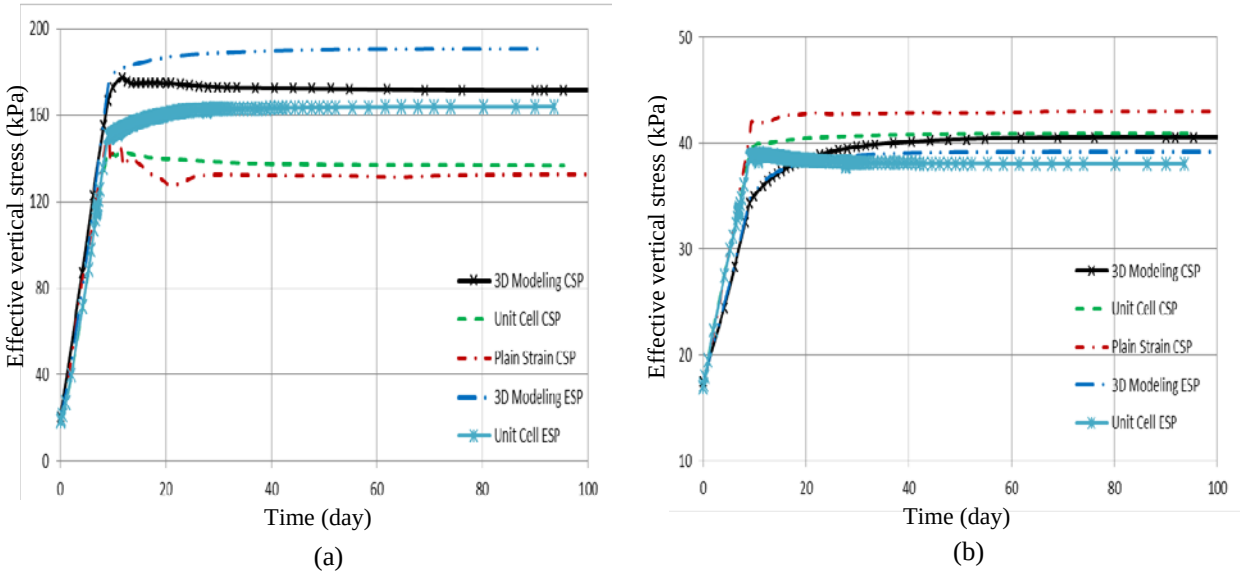

Figure 8: Effective vertical stress in the top of (a) The pile close to the embankment centre

(b) The soil near the embankment centre

The total stress in the reinforced soft soil with the conventional and the encased stone piles was calculated at point A which is located at a depth of 3.5 m. The relationship of the total vertical stress with consolidation time is shown in Fig. 10. The total vertical stress in the reinforced soil increases during construction until reaching maximum value. Beyond the maximum value, the reinforced soil with conventional piles implies approximate constant values of total stress along consolidation which is pronounced in the plain strain model. While the total stress decreases along consolidation when reinforcing soft soil with encased piles. The values of the total stress along consolidation in the reinforced soil with encased piles are smaller than those of the reinforced soil with convectional piles. This is more cleared in the unit cell model. This phenomenon means that greater load at the beginning and then the load decreases along consolidation time. The reinforced soil induces some degree of preloading. This phenomenon is not found in the non-reinforced soft soil which normally has constant total stress during consolidation. The reduction in the total stress of the reinforced soft soil with encased stone pile is a result for the stress transfer from the soil and stress concentration in the piles (Elsawy 2013).

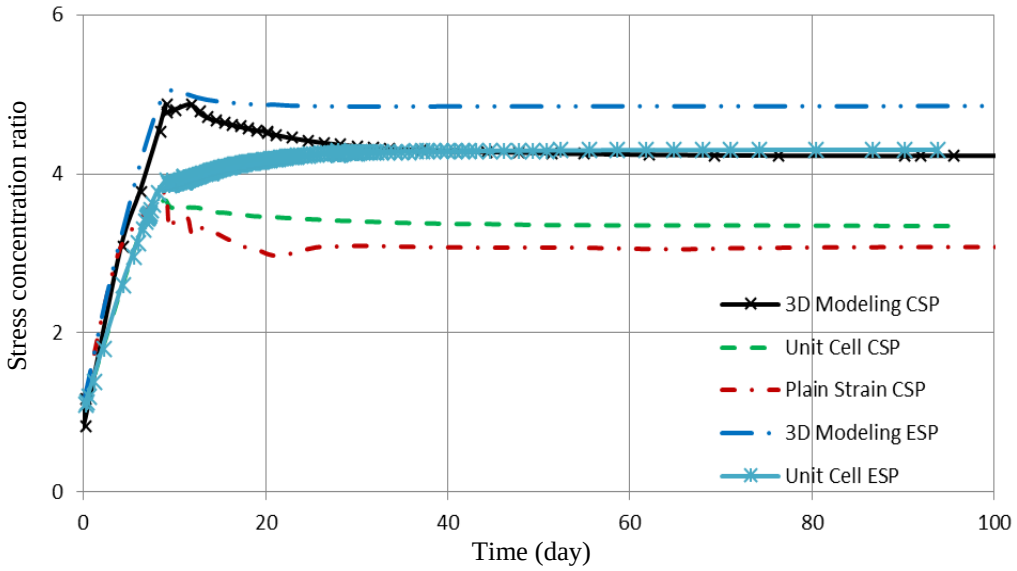

Figure 9: Stress concentration ratio at 1.0 m depth close the embankment centre

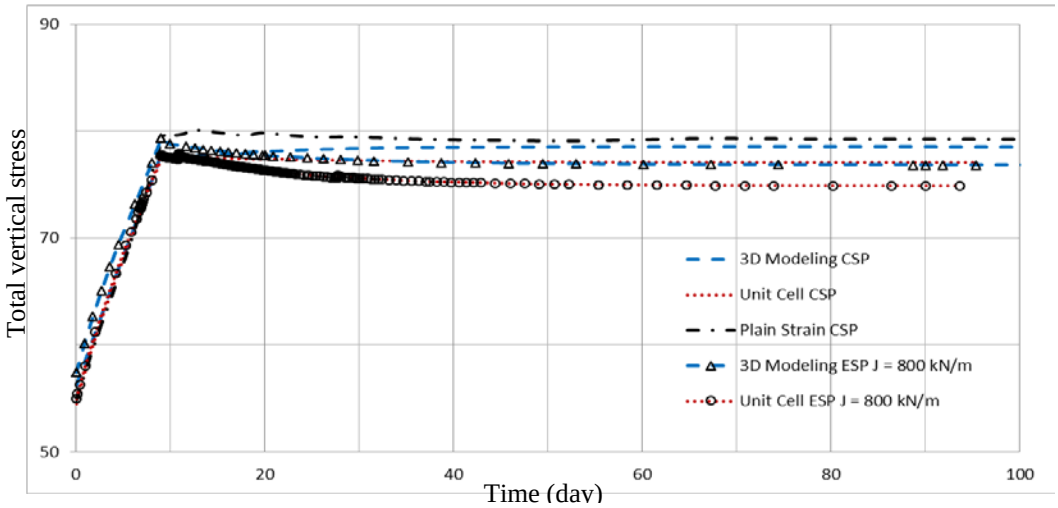

Figure 10: Total vertical stress in soil at point A

CONCLUSIONS

Construction of an embankment with 1.8 m height on reinforced soft soil with conventional stone piles is numerically simulated in the current study using the 3D, unit cell and plain strain models. The results of the numerical analyses are compared with the field measurement. The 3D and the unit cell models show a very good agreement with field measurement of the settlement while the plain strain model show overestimated results. The numerical analyses also investigated the behaviour of the reinforced soft soil with encased stone piles under the embankment. The stone piles are encased with geogrid material. The numerical results of the reinforced soil with conventional and encased piles show a very good agreement for the settlement between the 3D models and the unit cell model. The results of the excess pore water pressure imply a good agreement between all the used models. While the used models induce distant values of the stresses. This is more pronounced between the 3D model and the unit cell model. Moreover, the results of the numerical analyses indicate that:

1- Most of the consolidation settlement occurred at time of 35 days from construction. The reinforced soft soil with encased piles implies somewhat smaller settlement and consolidation time in comparison with the reinforced soft soil with conventional piles. The performance of the encased stone piles becomes better as developing consolidation time.

2- There is a small acceleration in the dissipation of the excess pore water pressure when reinforcing soft soil with encased piles. This is attributed to that the level of the applied load is somewhat low.

3- As the piles are encased, the stress concentration ratio increases. Additionally, the encasement of the piles doesn't only convert the softening in the effective stress of the pile to hardening but also do the vice versa in the effective stress of the surrounding soil. The pile encasement causes also reducing the total stress in the soil along consolidation which results in accelerating consolidation time.

REFERENCES

1. Ab Aziz, N. S., Jaheen, M., Mukri, M. and Ghani, A.: " Determination of the Ultimate Load of Encased Stone Column" *Electronic Journal of Geotechnical Engineering*, 2015 (20.22) pp 21493-12507. Available at ejge.com.
2. Almeida MSS, Hosseinpour I, Riccio M and Alexiew D (2014). Behavior of Geotextile-Encased Granular Columns Supporting Test Embankment on Soft Deposit. J. Geotech. Geoenviron. Eng. ASCE, ISSN 1090-0241/04014116.
3. Balaam, N. P. and Booker, I. R. (1985). Effect of stone column yield on settlement of rigid foundations in stabilized Clay. International Journal for Numerical and Analytical Methods in Ceomechanics 9, 331-351.
4. Bergado, D. T. and Long, P. V. (1994). Numerical analysis of embankment on subsiding ground improved by vertical drains and granular piles. Proceeding of the XIII ICSMFE, New Delhi, India, 1361-1366.
5. Borges, J. L., Domingues, T. S. and Cardoso, A. S. (2009). Embankments on soft soil reinforced with stone columns: numerical analysis and proposal of a new design method. Journal of Geotechnical and Geological Engineering 27, No. 6, 667-679.
6. Chandrawanshi, S., Kumar, R., Rokade, S., and Jain, P. K.: "Bearing Pressure and Settlement Analysis of Soft Ground Reinforced with Stone Columns". *Electronic Journal of Geotechnical Engineering*, 2016 (21.25) pp 1081-1094. Available at ejge.com.
7. Das P. and Pal UK. "A study of the behavior of stone column in local soft and loose layered soil" *Electronic Journal of Geotechnical Engineering* 2013 18 pp 1777–1786. Available at ejge.com.
8. Deb, K. (2010) A mathematical model to study the soil arching effect in stone column-supported embankment resting on soft foundation soil. Applied Mathematical Modelling 34 (2010) 3871–3883.
9. Elsawy, M. B. (2013). Behaviour of soft ground improved by conventional and geogrid-encased granular piles based on FEM study. Geosynth. Int., 20(4), 276-285.
10. FHWA (Federal Highway Administration). (1980). “Highway sub-drainage design manual.” Rep. TS-80-224, Washington, DC.
11. Gniel, J., and Bouazza, A. (2010). “Construction of geogrid encased stone columns: A new proposal based on laboratory testing.” Geotextile and Geomembrane 28(1), 108–118.
12. Hosseinpour, I., Almeida, M. S. S. and Riccio, M. 2015. Full-scale load test and finite-element analysis of soft ground improved by geotextile-encased granular columns, Geosynth. Int., 22, (6), 428–438, doi: 10.1680/gein.15.00023.
13. Khabbazian M, Kaliakin VN and Meehan CL (2015). Column Supported Embankments with Geosynthetic Encased Columns: Validity of the Unit Cell Concept. Geotech Geol Eng. 33:425–442.
14. Marto, A.; Moradi, R.; Helmi, F.; Latifi, N. and Oghabi, M. (2013) “Performance Analysis of Reinforced Stone Columns Using Finite Element Method”, *Electronic Journal of Geotechnical Engineering*, 2013 18B pp 315-323 Available at ejge.com

15. Mokhtari, M. and Kalantari, B.: "Soft Soil Stabilization using Stone Columns A review", *Electronic Journal of Geotechnical Engineering*, 2012 (17J) pp. 1459-1466. Available at ejge.com.

16. Murugesan, S., and Rajagopal, K. (2007). "Model tests on geosynthetic encased stone columns." Geosynth. Int., 14(6), 346–354.

17. Murugesan, S. and Rajagopal, K. 2010. Studies on the behavior of single and group of geosynthetic encased stone columns, Journal of Geotechnical and Geoenvironmental Engineering, 136, (1), 129–139.10.1061/(ASCE)GT.1943-5606.0000187.

18. Ng, K. S. and Tan, S. A (2014). Stress Transfer Mechanism in 2D and 3D Unit Cell Models for Stone Column Improved Ground. Int. J. of Geosynth. and Ground Eng. 1:3 DOI 10.1007/s40891-014-0003-1.

19. Raithel, M., Kempfert, H. G., and Kirchner, A. (2002). "Geotextile encased columns (GEC) for foundation of a dike on very soft soils." Proc., 7th Int. Conf. on Geosynthetics, Balkema, Nice, France, 1025–1028.

20. Tan SA, Tjahyono S, and Oo KK (2008) Simplified plane-strain modeling of stone-column reinforced ground. J Geotech Geoenviron Eng 134(2):185–194.

Notations:

γ_{us}	Unsaturated Density
γ_{sa}	Saturated Density
ν	Poison's ratio
E	Modulus of Elasticity
K_h	Horizontal Coefficient of Permeability
K_v	Vertical Coefficient of Permeability
ć	Cohesion
φ'	Angle of Internal Friction
CSP	Conventional Stone Piles
ESP	Encased Stone Piles

Editor's note.
This paper may be referred to, in other articles, as:

Mohamed B. D. Elsawy: "Conventional and Geogrid-encased Stone Piles Improved Soft Ground under an Embankment" Electronic Journal of Geotechnical Engineering, 2017 (22.09), pp 1561-1573. Available at ejge.com.